Period-doubling cascades and devil's staircases of the driven van der Pol oscillator

Ulrich Parlitz and Werner Lauterborn

Drittes Physikalisches Institut, Universität Göttingen D-3400 Göttingen, Federal Republic of Germany

(Received 12 February 1987)

Bifurcation diagrams of the driven van der Pol oscillator are given showing mode-locking and period-doubling cascades. At low driving amplitudes locking regions occur following Farey sequences. At high driving amplitudes this relationship is destroyed due to the appearance of period-doubling cascades and coexisting attractors. A generalization of the winding number is used to compute devil's staircases and winding-number diagrams of period-doubling cascades. The winding numbers at the period-doubling bifurcation points constitute an alternating sequence that converges at the accumulation point of the cascade.

I. INTRODUCTION

The van der Pol oscillator

$$\ddot{x}+d(x^2-1)\dot{x}+x=a\cos(\omega t)$$

or equivalently written

$$\begin{aligned}\dot{x}_1&=x_2\\ \dot{x}_2&=-d(x_1^2-1)x_2-x_1+a\cos(2\pi x_3)\ ,\\ \dot{x}_3&=\frac{\omega}{2\pi}\end{aligned}\tag{1}$$

is one of the most intensely studied systems in nonlinear dynamics.[1–14] It serves as a basic model of self-excited oscillations in physics, electronics, biology, neurology, and many other disciplines. Many efforts have been made to approximate the solutions of (1) (Refs. 2–9) or to construct simple maps that qualitatively describe important features of the dynamics.[10,11] Although some of these maps possess strange attractors no investigation of the original equation (1) concerning chaotic solutions is known to the authors. In this paper we therefore want to give examples of bifurcation diagrams of the driven van der Pol oscillator (1) showing, besides other features, complete period-doubling cascades. A new quantity called (generalized) winding number that has been introduced recently in connection with nonlinear resonances of driven dissipative oscillators[15] is used to describe the topological changes of the local flow around a period-doubling orbit. Furthermore we present a devil's staircase based on this (generalized) winding number and discuss its (fractal) dimension.

II. BIFURCATION DIAGRAMS

The following bifurcation diagrams show the strobed amplitude of the oscillations (i.e., projections of the attractors in the Poincaré cross section onto the coordinate X_{1p} of the cross section) versus the excitation frequency ω. The damping parameter is held constant at $d=5$. Figure 1 shows a bifurcation diagram for $a=1$ and $0<\omega<1.5$. Quasiperiodic and periodic oscillations (mode-locked states) occur. All trajectories lie on an invariant torus within the three-dimensional phase space.

Figure 2(a) shows the Poincaré cross section of a typical quasiperiodic attractor. The corresponding orbit $\{(x_{1p}^n,x_{2p}^n),n\in\mathbb{Z}\}$ of the Poincaré map is restricted to an invariant circle and may therefore be described by a one-dimensional circle map, called *attractor map*. The angles Θ_n of the orbit points $(x_{1p}^n,x_{2p}^n)(n=1,2,3,\dots)$ with respect to the origin within the invariant circle are used to parametrize the attractor map $\Theta_n\mapsto\Theta_{n+1}$. The graph of the map obtained in this way is shown in Fig. 2(b).

When the driving amplitude a is increased the periodic windows become larger. Figure 3 shows a bifurcation diagram for $a=2.5$. Between the ω intervals where mode locking with (small) odd periods 1,3,5,7,... takes place periodic orbits with large periods and quasiperiodic orbits occur. A section of Fig. 3 showing details of the parameter interval between the period-3 and the period-5 oscillations is given in Fig. 4. Numerical investigations of the other intervals (e.g., period-5 to period-7, period-7 to period-9, etc.) have shown that all intervals evolve in the

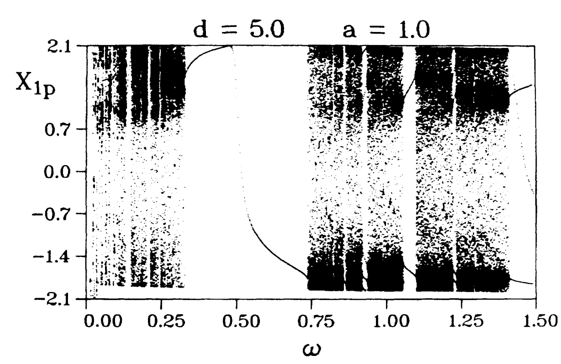

FIG. 1. Bifurcation diagram for $a=1$ showing the first coordinate X_{1p} of the attractor in the Poincaré cross section versus the excitation frequency ω that has been increased in small steps. After each step the last solution has been used as new initial value. All oscillations with even periods occur by pairs, where only one of the coexisting attractors is plotted here and in the following diagrams.

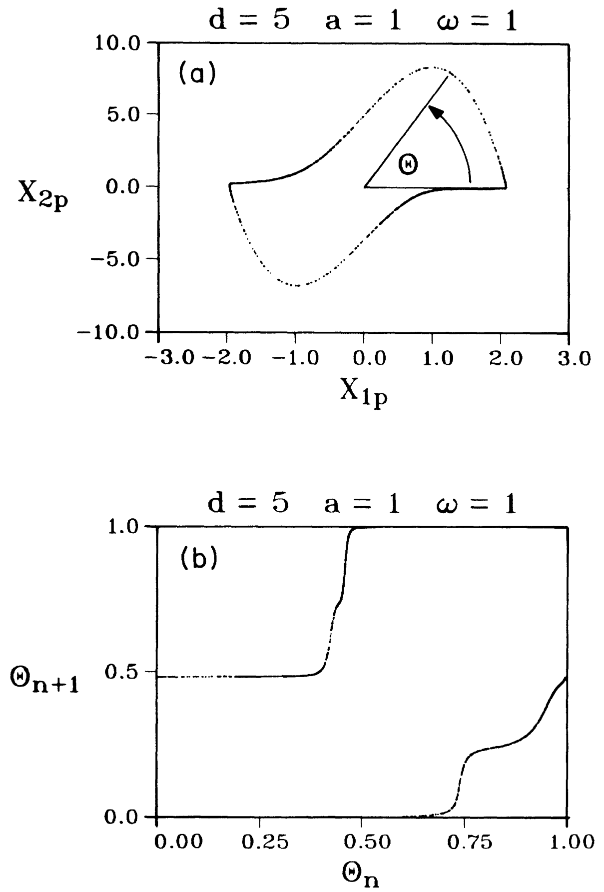

FIG. 2. (a) Poincaré cross section of an attractor lying on an invariant torus in phase space. (b) Attractor map of the attractor shown in Fig. 2(a).

same way, when the excitation amplitude a is varied. This phenomenon is similar to the superstructure observed in the bifurcation sets of the Duffing equation,[15,16] the Toda oscillator,[17] and the driven pendulum.[18] The superstructure of the bifurcation set of a driven nonlinear oscillator arranges a specific fine structure of bifurcation curves (surfaces) in the parameter space in a repetitive order that is closely connected with the nonlinear resonances of the system. The ω interval shown in Fig. 4 may be viewed as a prototype of all the other intervals between the entrainment regions with (small) odd periods occurring in Fig. 3.

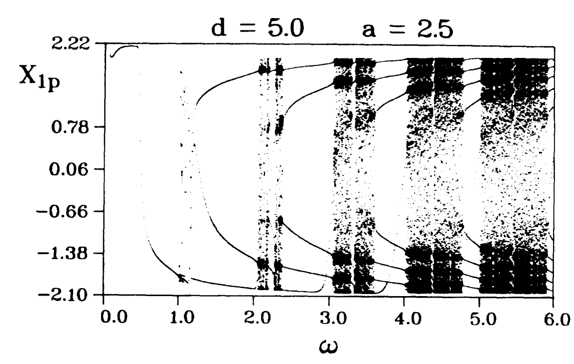

FIG. 3. Bifurcation diagram for $a=2.5$ (compare Fig. 1). Between the extended locking regions of period 1,3,5,7,. . . parameter intervals with large-period oscillations occur each of them undergoing the same bifurcation scenario when the excitation amplitude a is increased.

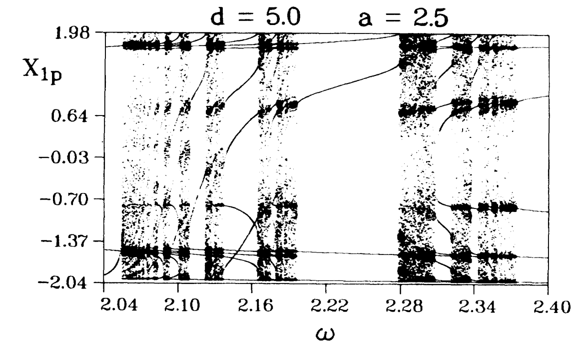

FIG. 4. Bifurcation diagram for $a=2.5$, showing an enlarged section of the bifurcation diagram given in Fig. 3. The parameter interval between the period-3 and the period-5 oscillation given here may be viewed as a prototype of all the large-period intervals in Fig. 3.

As the van der Pol oscillator is a symmetric system oscillations with even periods must occur as pairs of two asymmetric coexisting solutions.[19] In all bifurcation diagrams given here only one of these two partner orbits is plotted. The coexistence of asymmetric attractors is a feature of the van der Pol oscillator that differs from the scenario of the ordinary sine circle map.[20] Figure 5 shows the largest Lyapunov exponent of the Poincaré map versus the driving frequency ω. It is nonpositive in the whole ω interval, i.e., no chaotic states occur in this parameter range. A similar investigation of the larger ω interval shown in Fig. 3 led to the same result.

III. GENERALIZED WINDING NUMBERS

Besides bifurcation diagrams plots showing the winding number in dependence on the excitation frequency are very useful to analyze the complicated parameter dependence of mode-locked oscillations. In Ref. 5 we introduced a definition of a winding number based on the torsion of the local flow around a given orbit. In contrast to

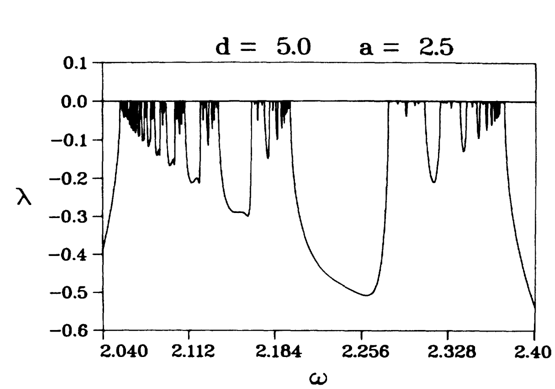

FIG. 5. Largest Lyapunov exponent λ_{max} versus driving frequency ω (compare Fig. 4 and Fig. 7).

the ordinary definition of the winding number[13,14] this local concept does not need an invariant torus in phase space. In the following we briefly want to motivate the definition of this new quantity. Let γ be an orbit of the van der Pol oscillator associated with the solution $x(t)=(x_1(t),x_2(t),x_3(t))$ of equation (1) and let γ' be a neighboring orbit of γ given by the solution $z(t)=x(t)+y(t)$ of (1). The perturbation $y(t)$ is assumed to be (infinitesimally) small. Then the local torsion of the flow is described by the rotations of the difference vector $y(t)$ about γ (compare Fig. 6). The time evolution of $y(t)$ is given by the variational equation (2) of (1)

$$\begin{aligned} \dot{y}_1 &= y_2 , \\ \dot{y}_2 &= -(2dx_1x_2+1)y_1 - d(x_1^2-1)y_2 , \\ \dot{y}_3 &= 0 . \end{aligned} \tag{2}$$

To describe the torsion of the local (i.e., linearized) flow only the first two equations of (2) are of importance (because $y_3=\text{const}$). Using polar coordinates $(y_1,y_2)=(r\cos\alpha, r\sin\alpha)$ we obtain the (reduced) variational equations in polar coordinates (3)

$$\begin{aligned} \dot{r} &= r\{[1-(2dx_1x_2+1)]\sin\alpha\cos\alpha \\ &\quad -d(x_1^2-1)\sin^2\alpha\} , \\ \dot{\alpha} &= -(2dx_1x_2+1)\cos^2\alpha - d(x_1^2-1)\sin\alpha\cos\alpha \\ &\quad -\sin^2\alpha . \end{aligned} \tag{3}$$

The mean angular velocity Ω of the difference vector $y(t)$ is given by

$$\Omega(\gamma) = \lim_{t\to\infty} \frac{1}{t}\int_0^t \dot{\alpha}\, dt' = \lim_{t\to\infty} \frac{\alpha(t)-\alpha(0)}{t} . \tag{4}$$

We call $\Omega(\gamma)$ the *torsion frequency* of the orbit γ. From (2) it is easy to see that $\Omega(\gamma)$ is always negative. We use the torsion frequency Ω_h of the driving harmonic oscillator

$$\Omega_h = -\omega \tag{5}$$

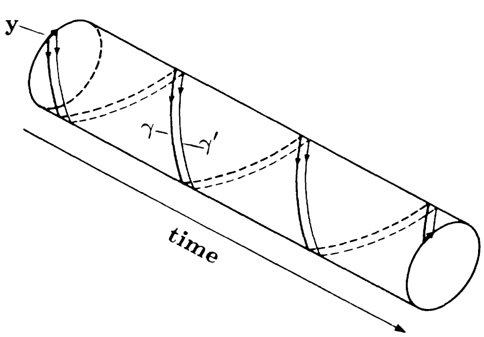

FIG. 6. A trajectory γ and its neighboring orbit γ'. The torsion frequency measures the mean rotation frequency of the difference vector y with respect to γ. If the attractor lies on an invariant torus the generalized winding number (6) equals the ordinary winding number because the number of "windings" of the trajectory γ equals the number of rotations of the difference vector y.

to define the *winding number* $w=w(\gamma)$ as

$$w(\gamma) = \frac{\Omega(\gamma)}{\Omega_h} . \tag{6}$$

The quantity w is called winding number because it equals the ordinary winding number as long as an invariant torus exists (compare Fig. 6). Especially in those cases where the (Poincaré) cross section of the torus differs strongly from the shape of a circle w is much easier to compute than the ordinary winding number. Therefore definition (6) may be useful for the investigation of conservative systems, too. An alternative derivation of (4) using the *QR* decomposition of the linearized flow map and further details can be found in Ref. 15. In contrast to already existing concepts of winding or rotation numbers our winding number w is also well defined for systems that do not possess an invariant torus in phase space or where the torus is broken. It enables the description of physical systems with coexisting attractors and the definition of winding numbers of strange attractors. We conjecture that in the case of chaos the limit (4) exists in the same sense and under the same conditions as that of the Lyapunov exponents. For periodic oscillations with period (number) m we call

$$n = mw \tag{7}$$

the *torsion number* of the closed orbit γ. The torsion number is a suitable quantity to classify saddle node and period-doubling bifurcation curves (surfaces) in the parameter space of one-dimensional driven dissipative oscillators. Furthermore it may be used to give an exact definition of resonance that does not depend on the existence of an invariant torus.[15] We call a periodic oscillation *resonant* when it possesses an integer torsion number.[21]

IV. A DEVIL'S STAIRCASE

Figure 7 shows a winding-number diagram corresponding to the bifurcation diagram in Fig. 4. Every "step" on the "devil's staircase" is associated with a rational value of w. The numerator of this rational number w is the torsion number n of the orbit and the denominator its period m. A diagram showing the inverse period $1/m$ versus the excitation frequency is given in Fig. 8 to elucidate the

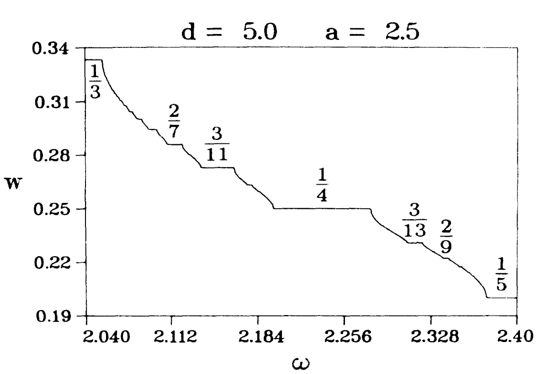

FIG. 7. Winding-number diagram for $a=2.5$ corresponding to Fig. 4 showing a devil's staircase.

self-similarity of the staircase. As can be seen from the diagrams in Fig. 7 and Fig. 8 the winding number in the locking region follows Farey sequences up to high order. Bak, Bohr, and Jensen[20] showed numerically that in the case of the one-dimensional sine circle map the complement of the locked states may become a fractal set with dimension $D=0.868\ldots$. In this case the staircase is called a complete devil's staircase. Meanwhile the value $D=0.868\ldots$ for the dimension of the complete devil's staircase has also been found in a hydrodynamical experiment[22] and other systems. A renormalization approach has confirmed the conjecture that this value of D is universal for a certain class of one-dimensional maps.[23] Unfortunately it is not easy to compare these results of the circle map theory with the corresponding scaling behavior of general systems such as the van der Pol oscillator. In the case of the circle map the critical curve in parameter space where the staircase becomes complete is a well-known straight line. In general, however, almost nothing is known about this curve. Even theorems concerning its smoothness features or algorithms to trace it do not seem to exist. Only some methods to locate it approximately in the parameter space are mentioned in the literature (e.g., Refs. 20 and 22). When we apply the technique described in Ref. 23 to the devil's staircase in Fig. 7 we obtain approximants D^n of the fractal dimension that range between 0.7 and 0.9. These results may be interpreted in a way that is compatible with the conjecture that $0.868\ldots$ is a universal dimension of complete devil's staircases of continuous systems, too. Details of this investigation will be given elsewhere.

V. PERIOD-DOUBLING CASCADES

When the excitation amplitude a is increased further the locking intervals in the diagram become wider and intervals with smaller periods compress or remove those with larger periods. Then the invariant torus is destroyed and symmetry breaking and (first finite) period-doubling cascades occur. Figure 9 shows a sequence of trajectories in the projection onto the (x_1,x_2) plane of the $\mathbb{R}^2\times S^1$ phase space. In Fig. 9(a) a symmetry-broken trajectory of (basic) period 4 is given. It successively period doubles to period 4×2 [Fig. 9(b)], period 4×2^2 [Fig. 9(c)], and to a chaotic orbit [Fig., 9(d)]. The Poincaré cross section of this chaotic attractor consists of four very thin islands. Figure 10 shows the Poincaré cross section of the chaotic attractor at $\omega=2.466$ (compare Figs. 11 and 12). A part of the attractor is blown up to emphasize its very thin structure. The Lyapunov dimension has been determined to $D_L=1.014$. Figure 11 shows a bifurcation diagram of this period-doubling cascade into chaos. In Fig. 12 an enlargement of the period-doubling cascade and diagrams of the corresponding Lyapunov exponents and winding numbers are given. In the period-doubling cascade the winding number is constant near bifurcation points.[15]

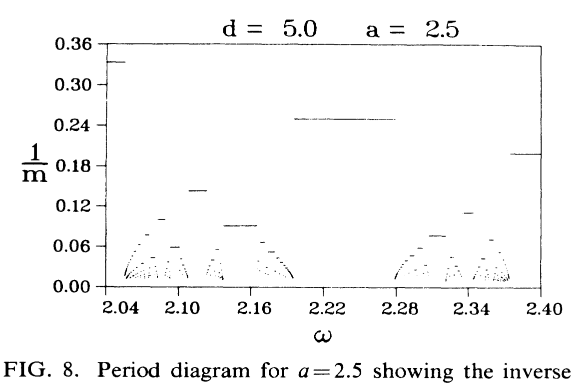

FIG. 8. Period diagram for $a=2.5$ showing the inverse $1/m$ of the period m of the oscillation vs the excitation frequency ω. (Compare Figs. 4, 5, and 7.)

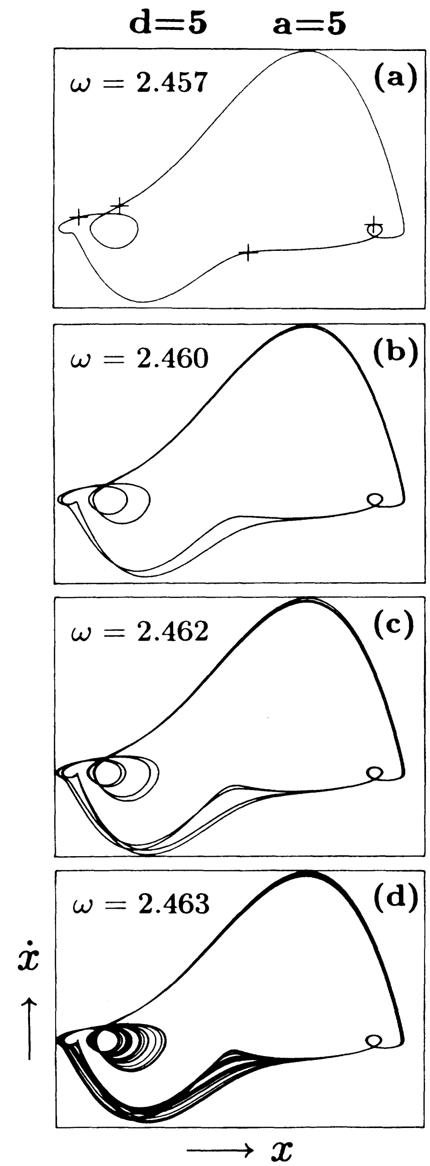

FIG. 9. Period-doubling sequence of a (basic) period-4 attractor. The damping parameter d and the driving amplitude a equal 5. (Compare Figs. 11 and 12). (a) Period-4 attractor. The orbit repeats after 4 periods of the driving as indicated by the crosses. (b) Period-4×2^1 attractor. (c) Period-4×2^2 attractor. (d) Period-4 chaos.

The height of these steps in the winding-number diagram is given by a simple formula similar to the result for the torsion number in a period doubling cascade.[15,24] At the kth period-doubling bifurcation point of the cascade shown in Fig. 11 the winding number w takes the value

$$w_k = w_\infty + \frac{(-1)^k}{3m_0 2^k} , \tag{8}$$

where w_∞ is the winding number at the accumulation point of the period-doubling cascade. w_∞ is given by the (basic) winding number w_0 and the (basic) period m_0 of the locking region (Arnold tongue) where the period-doubling cascade takes place,

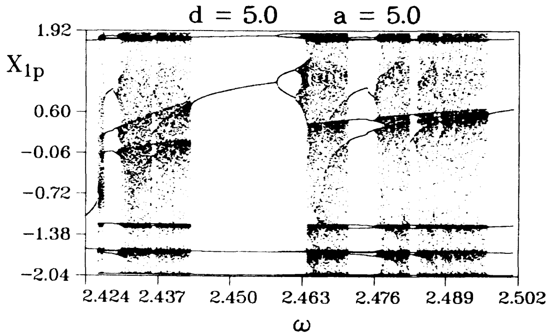

FIG. 11. Bifurcation diagram of the period-3 to period-5 interval for $a=5$ showing complete period-doubling cascades into chaos. Owing to the symmetry of the system for each period-doubling cascade a counterpart exists (which is reached from other intial conditions) that is not plotted here.

$$w_\infty = w_0 - \frac{1}{3m_0} . \tag{9}$$

The period doublings shown in Figs. 9 and 12 occur in the locking region with $w_0=\frac{1}{4}$ and $m_0=4$. Therefore w_∞ equals $\frac{1}{6}$ and the winding numbers are $w_1=\frac{1}{8}$, $w_2=\frac{3}{16}$, $w_3=\frac{5}{32}, \ldots$ (see Fig. 12). This parameter dependence of the winding number in a period-doubling

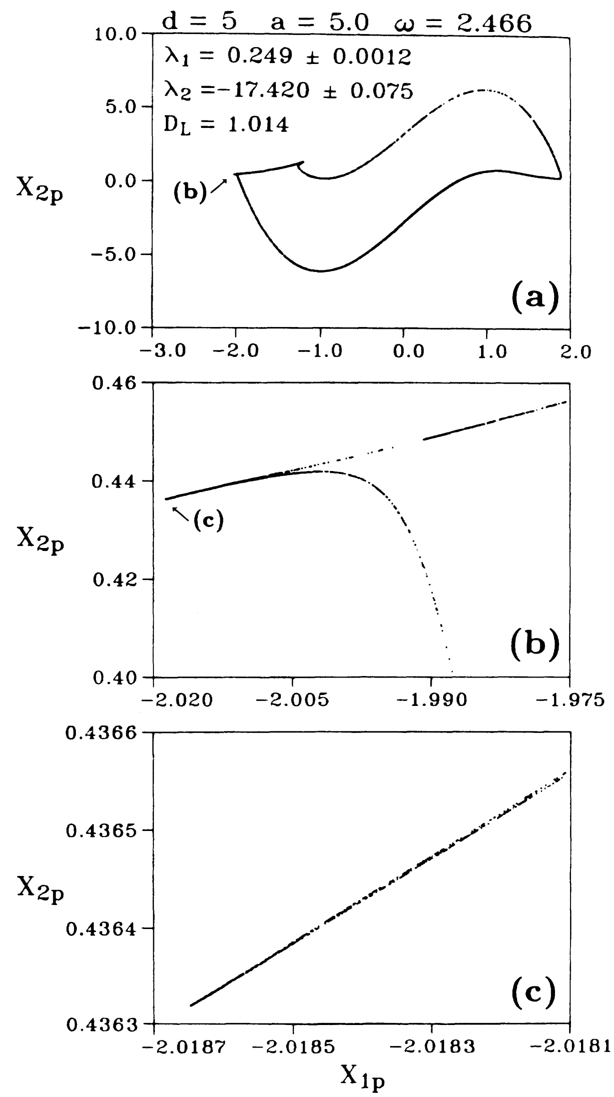

FIG. 10. Cross section of the strange attractor at $x_3=0$ for $d=5$, $a=5$, and $\omega=2.466$ (compare Figs. 11 and 12). Inserted in the plot of the whole attractor (a) are the Lyapunov exponents λ_1 and λ_2 of the Poincaré map and the Lyapunov dimension D_L which equals almost one. This very small value of D_L is consistent with the very thin structure of the attractor shown in the enlargements (b) and (c).

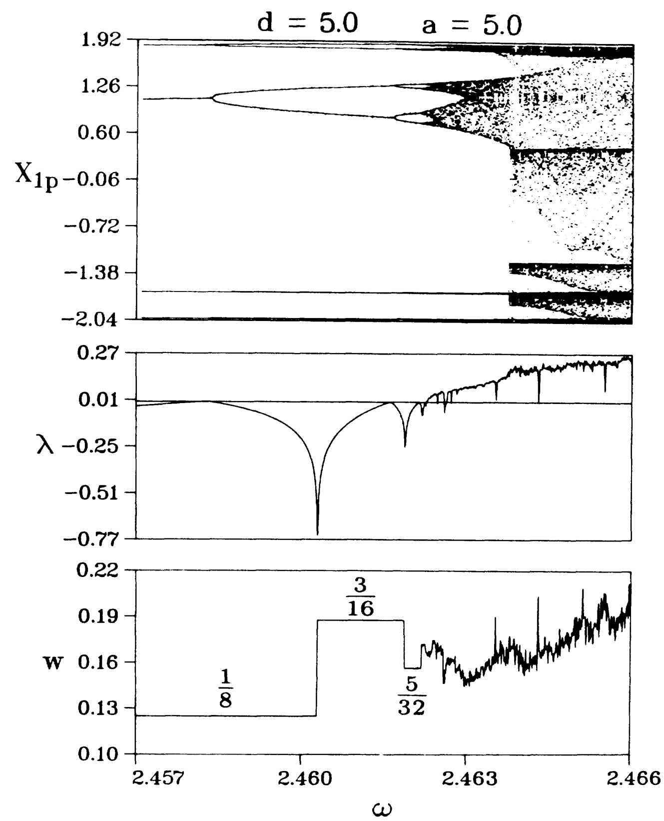

FIG. 12. Enlargement of the bifurcation diagram shown in Fig. 8 and the corresponding evolution of the largest Lyapunov exponent λ and the winding number w.

cascade describes the evolution of the invariant manifolds of the attractor.[17,24] Some period-doubling cascades of the van der Pol oscillator (e.g., the period-13×2^n cascade between $\omega=2.4711$ and 2.4765 in Fig. 11 with $w_0=\frac{2}{13}$, $w_1=\frac{5}{26}, w_2=\frac{9}{52},\ldots$) do not obey the law (8) but instead the very similar formula,

$$w_k = w_\infty - \frac{(-1)^k}{3m_0 2^k}\,, \qquad w_\infty = w_0 + \frac{1}{3m_0}\,. \tag{10}$$

The two (empirical) recursion schemes (8) and (10) apply to the period-doubling cascades of many other nonlinear oscillators, too.[17,25] That two kinds of winding-number sequences occur may be understood by looking at the logistic map. There the winding number is simply given as the relative number of R's in the $R-L$ string of the symbolic description of the dynamics, and the formulas (8) and (10) are immediate consequences of the construction law for the symbolic strings upon period doubling. Beyond the accumulation point of the period-doubling cascade the winding number describes the geometry of the strange attractor. Details will be given in a forthcoming paper.[25]

At even higher excitation amplitudes the bifurcation diagram becomes very complicated due to a multitude of coexisting attractors and period doubling cascades. As an example, Fig. 13 shows a bifurcation diagram for $a=40$. At $\omega=5.06\ldots$ the period-1 attractor undergoes a Hopf bifurcation and an invariant torus in phase space is created. In those parts of the diagram where period-doubling cascades occur the torus is destroyed again or the period-doubling attractors coexist with the torus. A detailed investigation of this part of the parameter space will probably yield further interesting results.

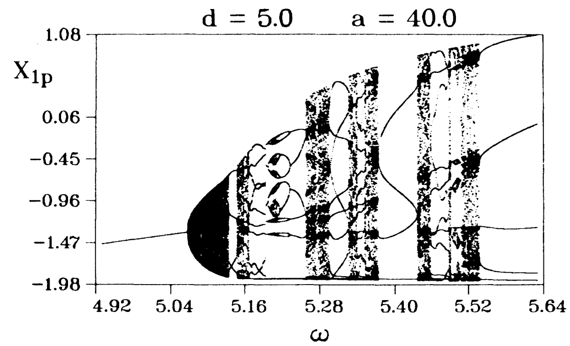

FIG. 13. Bifurcation diagram for $a=40$. A Hopf bifurcation and period-doubling cascades occur.

VI. CONCLUSION

Mode-locking phenomena and period-doubling cascades of the driven van der Pol oscillator have been investigated. In both cases a new quantity called (generalized) winding number was used to describe the dynamical behavior of the system and its parameter dependence. As long as all attractors lie on an invariant torus the winding-number diagrams show the well-known devil's staircase scenario. For large driving amplitudes, however, the invariant torus may be destroyed and period-doubling cascades into chaos occur. The winding number w_k at the period-doubling points constitute an alternating sequence converging at the accumulation point of the period-doubling cascade. This sequence describes the folding and unfolding process of the invariant manifolds.[17,24] For large driving amplitudes the Farey ordering is destroyed and many periodic, quasiperiodic, and chaotic attractors coexist. Details of this part of the parameter space will be published elsewhere.

ACKNOWLEDGMENTS

This work was supported by the Stiftung Volkwagenwerk. We thank the members of the Nonlinear Dynamics Group at the Third Physical Institute of the University of Göttingen, especially T. Kurz, K. Geist, and M. Wiesenfeldt, for many valuable discussions. All computations have been carried out on a SPERRY 1100 and a VAX-11/780 of the Gesellschaft für wissenschaftliche Datenverarbeitung, Göttingen.

[1]B. van der Pol, Philos. Mag. **43**, 700 (1927).
[2]M. L. Cartwright and J. E. Littlewood J. London Math. Soc. **20**, 180 (1945).
[3]E. M. El-Abbasy, Proc. R. Soc. Edinburgh Sect. A **100**, 103 (1985).
[4]N. Levinson, Ann. Math. **50**, 127 (1949).
[5]J. P. Gollub, T. O. Brunner, and B. G. Danly, Science **200**, 48 (1978).
[6]P. J. Holmes and D. A. Rand, Q. Appl. Math. **35**, 495 (1978).
[7]J. Grasman, E. J. M. Veling, and G. M. Willems, SIAM (Soc. Ind. Appl. Math.) J. Appl. Math. **31**, 667 (1976).
[8]J. Grasman, M. J. W. Jansen, and E. J. M. Veling, North Holland Math. Studies **31**, 93 (1978).
[9]J. Grasman, Q. Appl. Math. **38**, 9 (1980).
[10]J. Guckenheimer, Physica **1D**, 227 (1980).
[11]J. Grasman, N. Nijmeijer, and E. J. M. Veling, Physica **13D**, 195 (1984).
[12]J. E. Flaherty and F. C. Hoppensteadt, Stud. Appl. Math. **58**, 5 (1978).
[13]J. Guckenheimer and P. J. Holmes, *Nonlinear Oscillations, Dynamical System, and Bifurcations of Vector Fields* (Springer, Berlin, 1983).
[14]H. G. Schuster, *Deterministic Chaos* (Physik Verlag, Weinheim, 1984).
[15]U. Parlitz and W. Lauterborn, Z. Naturforsch. **41A**, 605 (1986).
[16]U. Parlitz and W. Lauterborn, Phys. Lett. **107A**, 351 (1985).
[17]T. Kurz and W. Lauterborn (unpublished).
[18]K. Schmidt and H. G. Schuster (unpublished).
[19]J. W. Swift and K. Wiesenfeld, Phys. Rev. Lett. **52**, 705 (1984).
[20]M. H. Jensen, P. Bak, and T. Bohr, Phys. Rev. A **30**, 1960

(1984).
[21]In Ref. 15 we proposed as resonance criterion the existence of a rational winding number (5). That definition also included all cases where the torsion number is a noninteger rational number. The inclusion of this possibility was not intended.
[22]J. Stavans, F. Heslot, and A. Libchaber, Phys. Rev. Lett. **55**, 596 (1985).
[23]P. Cvitanovic, M. H. Jensen, L. P. Kadanoff, and I. Proccacia, Phys. Rev. Lett. **55**, 343 (1985).
[24]P. Beiersdorfer, Phys. Lett. **100A**, 379 (1984).
[25]U. Parlitz and W. Lauterborn (unpublished).